Solar activity and large geomagnetic disturbances

S. C. Dubey[†] and A. P. Mishra*

Department of Physics, Government Girl's College, Sidhi 486 661, India
*Department of Physics, A.P.S. University, Rewa 486 003, India

Various types of solar dynamic phenomena occurring on the solar surface are responsible for interplanetary and geomagnetic disturbances. A solar phenomenon known as coronal mass ejection (CME) is known to be responsible for major interplanetary disturbances and large geomagnetic storms. In the present study, we have analysed large geomagnetic storms associated with storm time index (D_{st}) decrease of more than 100 nT observed during the solar maximum of solar cycle 22 peaking around the year 1989, to find their association with CMEs and interplanetary disturbances (IPDs). We find that 90% large geomagnetic storms were associated with CMEs which cause the supersonic IP shocks in solar wind streams. The association of different interplanetary parameters with geomagnetic storms on the basis of two case studies has been discussed.

THE geomagnetic activity is generally represented by the electromagnetic coupling, $V \times B$, where V is the velocity of solar wind streams and B is the IMF magnitude. Two types of solar wind streams: corotating flows and transient disturbances produce two kinds of geomagnetic storms, termed as sudden commencement and gradual commencement storms. The north–south component of IMF B_z plays a dominant role in determining the amount of solar wind energy to be transferred to the geomagnetosphere[1,2]. When the IMF has a large magnitude ($\geq$ 10 nT) and a large southward component, the amount of transferred energy becomes very large. On the other hand, the transferred energy becomes very small when the IMF is directed preliminarily northward. The energy transfer efficiency is of the order of 10% during intense magnetic storms[3]. Viscous interaction, the other prime energy transfer mechanism proposed, has been shown to be only < 1% efficient during intense northward directed IMFs. Tsurutani *et al.*[4] have examined the interplanetary and solar causes of five largest geomagnetic storms during the period 1971–1986 and found that the extreme value of the southward IMF B_z, rather than the solar wind speeds, are the primary causes of great magnetic storms.

About two decades ago large coronal eruptions, now known as coronal mass ejections (CMEs), were discovered in coronagraph observations on the OSO-7 and Skylab spacecrafts[5,6]. The CMEs are vast structures of solar plasma and magnetic fields which are expelled from the Sun into the heliosphere and make a prime link between solar–interplanetary and geomagnetic disturbances. CMEs are now considered by many researchers as the solar origin of interplanetary disturbances (IPDs) and large geomagnetic storms. Large geomagnetic storms are often associated with CMEs and/or shocks in solar wind resulting from the interaction between high-speed and low-speed plasma streams[7]. In the light of previous work on CMEs, we have examined the association of large geomagnetic storms with CMEs during solar maximum year 1989. Different storm time changing phenomena have also been described.

In the present analysis, we have sorted out large geomagnetic storms associated with D_{st} decrease of more than 100 nT, IMF $B \geq 10$ nT with time duration greater than 3 h, during the year 1989. There were 20 such storms. We have established their association with CMEs on the basis of mass ejection speeds, nature of IPDs and kind of associative CME events. The data of equatorial D_{st} values and mass ejection from the Sun have been compiled from various volumes of Solar Geophysical Data (SGD) bulletins. The different solar wind velocity and interplanetary magnetic field data measured through a number of spacecraft/satellites have been compiled and reported for different periods by King[8]. The selected 20 large geomagnetic storms are listed in Table 1. One column contains the date of the observed storm. Another column presents the magnitude of the storm in nT. The different features of the storm and its related interplanetary parameters, such as types of storm, peak solar wind speed, peak value of IMF B, peak value of IMF B_z, types of IPDs and associative CME events are denoted in columns 3–8 respectively. There are many data gaps in the IMP data book, and so we introduce the symbol * for the data gap in Table 1.

Out of the 20 large geomagnetic storms, 13 are sudden storm commencement type and 7 are gradual storm commencement type. During the above-mentioned period, maximum number of large geomagnetic storms were associated with CMEs. Gosling *et al.*[7] have shown that all but one of the 37 largest geomagnetic storms in 1978–82 were associated with earth passage of either a shock disturbance or a CME or both. The results of our present study are similar to Gosling's results. According to many recent studies, CMEs can be associated with three types of solar activity, viz. H-alpha solar flares, eruptive prominences and X-ray bursts. The Skylab and SMM mission show that about 40% CMEs were associated with type-II and only 5% were associated with type-IV radio-bursts. These types of radio-bursts produce strong IP shocks which cause large geomagnetic storms on the earth. Our observations show that out of the large geomagnetic storms, 70% could be attributed

[†]For correspondence.

Table 1. Selected 20 large geomagnetic storms observed during the year 1989 and their associative interplanetary and solar features

Date of storm	Magnitude of storm (nT)	Type of storm	Maximum SWV (km/s)	Peak IMF B (nT)	Peak IMF B_z (nT)	Type of IPDs	Associative CME events
11/01/89	–132	G	744	25.9	–12.7	IP Shock	CMEs (II)
16/01/89	–122	G	685	13.9	–09.1	IP Shock	CMEs (II)
20/01/89	–122	S	*	*	*	*	CMEs (II)
09/03/89	–103	S	551	17.6	–08.8	IP Shock	CMEs (II)
14/03/89	–599	G	>839	*	*	*	CMEs (IV)
16/03/89	–118	G	743	22.7	–08.1	IP Shock	CMEs (II)
19/03/89	–110	G	880	22.7	–07.6	IP Shock	CMEs (IV)
29/03/89	–131	S	750	15.4	–09.8	IP Shock	CMEs (IV)
14/04/89	–105	S	458	15.1	–11.5	IP Shock	*
26/04/89	–132	S	646	22.5	–15.3	IP Shock	CMEs (II)
10/06/89	–144	S	>523	*	*	*	*
15/08/89	–146	S	667	32.7	–25.3	IP Shock	CMEs (IV)
29/08/89	–153	S	456	21.1	–16.3	M Cloud	CMEs (II)
16/09/89	–125	S	*	*	*	*	CMEs (II)
19/09/89	–257	S	*	*	*	*	CMEs (IV)
26/09/89	–157	S	>374	*	*	*	CMEs (II)
21/10/89	–270	G	918	33.5	–19.7	IP Shock	CMEs (IV)
13/10/89	–124	G	497	15.0	–12.8	IP Shock	CMEs (II)
17/11/89	–266	G	*	*	*	*	CMEs (II)
31/12/89	–104	S	672	18.4	–14.2	IP Shock	CMEs (II)

S, sudden commencement storms; G, gradual commencement storms; CMEs (II), CMEs associated with type-2 radio-burst; CMEs (IV), CMEs associated with type-4 radio-burst; *, sources are uncertain.

Table 2. Various solar events observed during 22–29 April 1989

Date	Time (UT)	Duration (min)	Associated solar events
22/4/89	03:47	4	CME (type-II)
22/4/89	06:00	5	CME (type-II)
22/4/89	06:55	18	CME (flare surge)
22/4/89	08:23	5	Solar flare (Imp – 1B)
23/4/89	07:20	40	CME (flare surge)
23/4/89	08:35	105	CME (flare surge)
23/4/89	21:55	1	CME (type-II)
23/4/89	23:55	49	Solar flare (Imp – 1B)
23/4/89	08:48	47	CME (flare surge)
23/4/89	07:18	17	CME (flare surge)

to type-II radio-burst and 30% to type-IV radio-burst. These results indicate that the large geomagnetic storms are generally associated with CMEs during solar maximum. The CME-associated large geomagnetic storms are either associated with type-II or type-IV radio-bursts.

In the present analysis, we describe a large geomagnetic storm observed during 25 April–1 May 1989. This storm is sudden commencement type having peak magnitude of 132 nT, initial phase duration of 7 h, main phase duration of 13 h and recovery phase duration of 130 h. During the main phase of this storm, solar wind speed and IMF magnitude peaking were around 661 km/s and 22.5 nT, respectively. The northward IMF B_z turned its value from 4.8 to –11.6 before the onset of main phase. The solar origin of this storm is CMEs type-II radio-burst which occurred during (03:47–03:51 and 06:00–06:05 UT) on 22 April 1989. Solar events that occurred during the period 22–29 April 1989, are listed in Table 2. This has a long longevity and many small peaks.

The association of the above-mentioned geomagnetic storm with different interplanetary parameters is plotted in Figure 1. From this plot, we notice that the initial phase of the geomagnetic storm starts when IMF B has low magnitude and IMF B_z is initially northwards. The main phase of geomagnetic storm starts with the increase in IMF B magnitude and solar wind speed, and turning of IMF B_z from north to south. The magnitude of this storm peaks 9 h after the IMF peak. During large recovery phase duration (130 h) of this storm, IMF B magnitude shows decreasing trend while solar wind speed shows increasing trend. The large southward IMF B_z is present during recovery phase. We conclude that the large solar wind velocities in the presence of even moderate southward IMF B_z can extend the recovery phase of the storm to around 130 h by maintaining the D_{st} values as high as –60 nT. This would not have been possible in the presence of northward IMF B_z, in spite of high solar wind velocities. For better understanding of this result, we have described another geomagnetic storm observed during 8–12 July 1991, shown in Figure 2. This storm is similar to the previous case, but has the presence of a large northward IMF B_z during

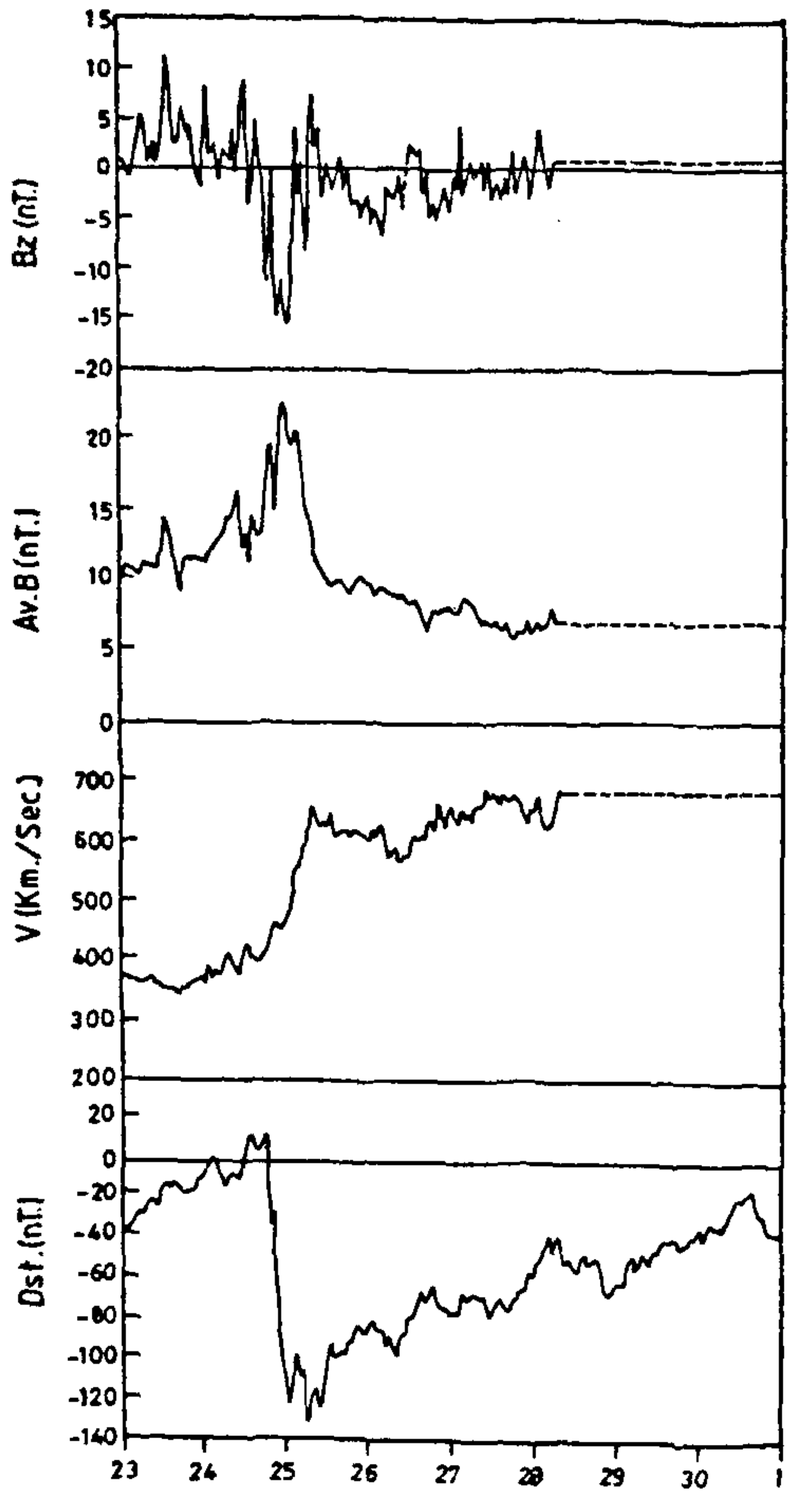

Figure 1. Association of geomagnetic storm with solar wind speed, interplanetary magnetic field IMF B and IMF B_z observed during 25 April–1 May 1989.

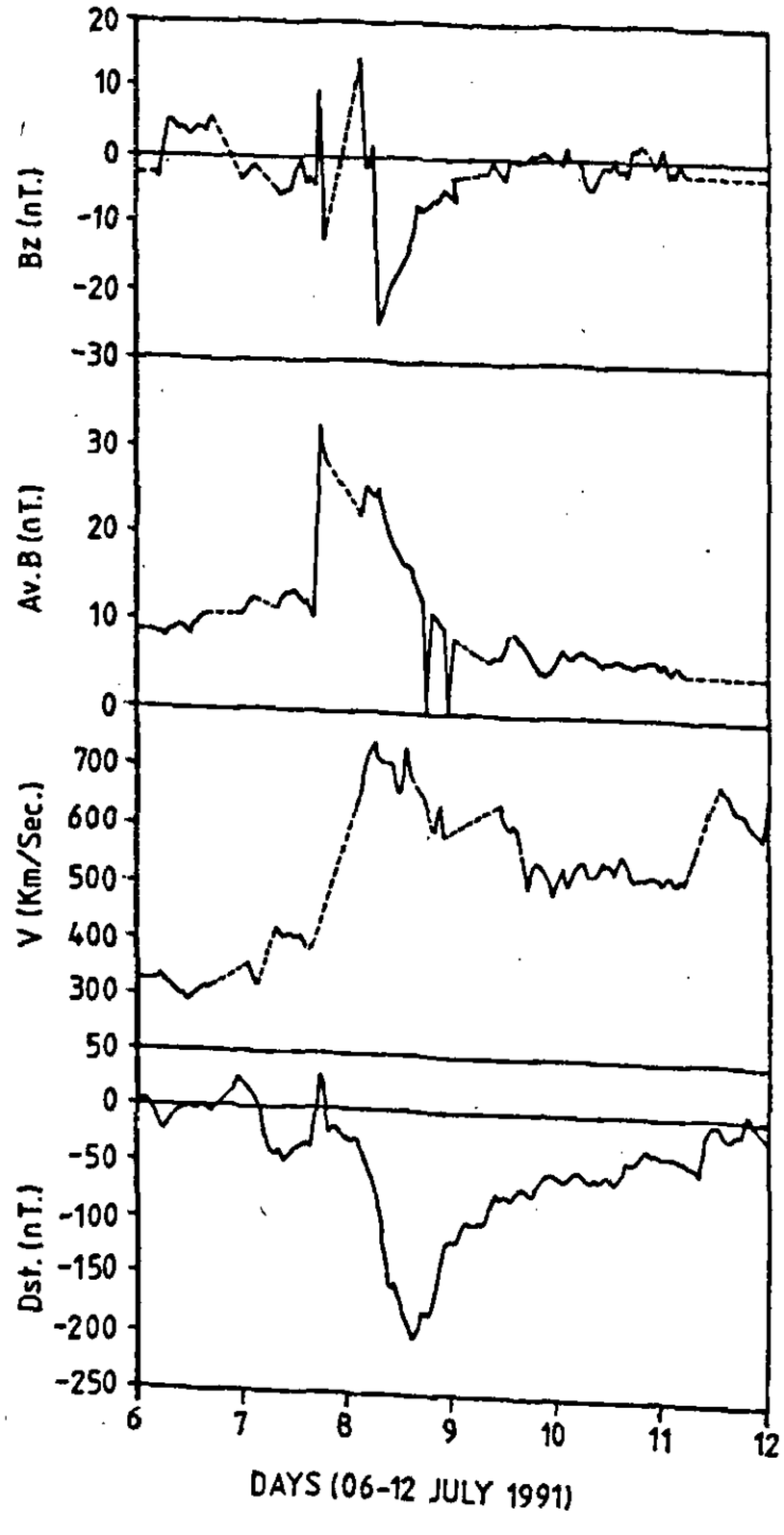

Figure 2. Association of geomagnetic storm with solar wind speed, interplanetary magnetic field IMF B and IMF B_z observed during 8–12 July 1991.

recovery phase. During the recovery phase of this storm comparatively higher magnitude (–198 nT) in comparison as in the previous case recovered within 69 h in the presence of higher solar wind velocity. Many recent studies have shown that the magnitudes and different phases of the geomagnetic storm depend upon solar wind speed, IMF magnitude and the presence of large southward IMF B_z. Actually southward IMF B_z provides an opportunity to make strong magnetic reconnection between IMF and the earth's magnetic field. The presence of large southward IMF B_z during higher solar wind velocities can produce large geomagnetic storms; it can extend the recovery phase of the storm and *vice versa*.

Geomagnetic storms are either caused by supersonic shocks or magnetic clouds. Supersonic shocks are caused by interaction of forward and reverse shock pairs in interplanetary medium where the magnetic clouds are transient ejections in the solar wind streams defined by relatively strong magnetic fields, the smooth magnetic field vector is higher than the average, and a low proton beta and proton temperature[9]. The magnetic field configuration in magnetic clouds is approximately force-free[10]. In our study period, 12 geomagnetic storms were associated with supersonic IP shocks while only one geomagnetic storm was associated with magnetic clouds. The IMF sources are uncertain for 7 geomagnetic storms due to data gaps in interplanetary medium data book. This analysis shows that the majority of geomagnetic storms were associated with IPDs caused by flow of supersonic IP shocks in comparison to magnetic clouds-associated geomagnetic storms, whereas magnetic clouds-associated geomagnetic storms contained higher IMF magnitude for longer duration in comparison to other IP shocks-associated geomagnetic storms. It seems that the magnetic clouds-associated geomagnetic storms could not contain higher magnitude. These results indicate that the presence of higher IMF for longer durations are not necessarily more effective for producing large magnitude geomagnetic storms.

1. Arnold, R., *J. Geophys. Res.*, 1971, **76**, 5189.

2. Akasofu, S. I., *Space Sci. Rev.*, 1981, **28**, 121.
3. Gonzalez, W. D., Tsurutani, B. T., Gonzalez, A. L. C., Smith, E. J., Tang, F. and Akasofu, S.-I., *J. Geophys. Res.*, 1989, **94**, 8835.
4. Tsurutani, B. T., Gonzalez, W. D., Tang, F. and Lee, *Geophys. Res. Lett.*, 1992, **19**, 73.
5. Tousey, R., in *Space Research XIII* (eds Rycroft, M. J. and Runcorn, S. K.), Akademie Verlag, Berlin, 1973, p. 173.
6. Gosling, J. T., *J. Geophys. Res.*, 1974, **79**, 4581.
7. Gosling, J. T., McComas, D. J., Phillips, J. L. and Bame, S. J., *J. Geophys. Res.*, 1991, **96**, 7831.
8. King, J. H., *Interplanetary Medium Data Book*, NSSDC, GSFC, Greenbelt, Maryland, 1994, Supplement 5.
9. Burlaga, L. F., Sittler, E., Mariani, F. and Schwenn, R., *J. Geophys. Res.*, 1981, **86**, 6673.
10. Goldstein, H., *NASA Conf. Publ.*, 1983, **731**, 2280.

ACKNOWLEDGEMENTS. We thank the anonymous referees for their valuable comments to improve this paper.

Received 7 September 1998; revised accepted 19 April 1999

Some new observations on the Amritpur Granite Series, Kumaun Lesser Himalaya, India

Prabha Pandey[†,§] and R. S. Rawat*

[†]National Geophysical Research Institute, Hyderabad 500 007, India
*Wadia Institute of Himalayan Geology, Dehradun 248 001, India

The Precambrian Amritpur Granite Series (AGS) in the Kumaun Lesser Himalaya is a composite body of three distinct types, viz. Porphyritic Amritpur Granite (PAG), Equigranular Amritpur Granite (EAG) Amritpur Porphyry (AP) and extends for a length of 60 km. Signature of Precambrian, pre-Himalayan contact metamorphism in addition to the Himalayan regional metamorphism (greenschist to lower amphibolite facies) and subsequent retrograde metamorphism are observed in the AGS. The authors have provided definite evidence for a contact aureole zone around AGS in the east of Hairakhan, NE of Durgapipal and Chandadevi and reported the xenoliths of PAG and EAG types in AP at Jamrani indicating a younger age of AP.

THE Amritpur Granite Series (AGS) is intrusive into the Bhimtal–Bhowali Formation (quartzite-metabasic association) and occurs in juxtaposition with the Siwaliks along the Main Boundary thrust (MBT), in the outer Kumaun Lesser Himalaya. The AGS is divisible into Porphyritic Amritpur Granite (PAG), Equigranular Amritpur Granite (EAG) and Amritpur Porphyry (AP[1], Figure 1 *a*). These three types are well exposed along the Gola river section (Figure 1 *b*). A lithotectonic set up of the area is presented in Table 1.

[§]For correspondence.

PAG has unassimilated to assimilated xenoliths of metavolcanics and quartzites (Figure 2 *a*). The assimilation of metabasic xenoliths in PAG has imparted a pink colouration to the K-feldspars (Figure 2 *b*). The metabasic xenoliths have provided necessary Mg and Fe which under the influence of Himalayan orogeny have been redistributed (because of fluids during deformation and metamorphism). The xenoliths of PAG and EAG are present in AP, indicating that the origin of AP was later than PAG and EAG (Figure 2 *c*).

The PAG has large phenocrysts of microcline/microcline microperthite (triclinicity varies from 0.604 to 0.833)[2] in the groundmass of subidiomorphic quartz, K-feldspar, microcline perthite, plagioclase, micas (biotite > muscovite), chlorite with zircon, apatite, tourmaline, sphene and monazite as accessory phases. The EAG shows hypidiomorphic (granitic) texture. It has quartz, K-feldspar, perthite, plagioclase with mica (muscovite > biotite), chlorite and tourmaline with the accessory phases (zircon, apatite, sphene and leucoxene). The AP has embayed grains of quartz and feldspar (plagioclase > K-feldspar) in the groundmass of quartz, K-feldspar, plagioclase, biotite, chlorite, penninite,

Table 1. The generalized litho-tectonic set up of the area (modified after Nautiyal and Rawat[11])

..... Ramgarh Thrust	
Bhimtal–Bhowali Formation	Metabasic intrusives (dolerite) with sulphides near Saleri slates (grey, red and purple coloured) Metabasics (metavolcanics), Coarse grained to fine grained (amygdaloidal) and foliated with sulphides (south of Bhimtal), Quartzites including thin lenses of hematite bearing quartzites and calc silicates
..... Intrusive contact	
Amritpur Granite Series	Metabasic intrusions (dolerites) with sulphides (south of Saleri), Tourmaline pegmatites, Aplite, Amritpur Porphyry (with Siwalik patch at Chaporiya) including sulphides (west of Jawari), Equigranular Amritpur Granite, Porphyritic Amritpur Granite
..... Intrusive contact	
Bhimtal–Bhowali Formation	Mylonitized quartzites, metabasics and slates with calc silicates and sulphides (in metabasics)
..... Main Boundary Thrust (MBT)	
Siwalik Group	Carbonaceous shales, clays and indurated pebbly grey to cream coloured sandstones with thin coal seams